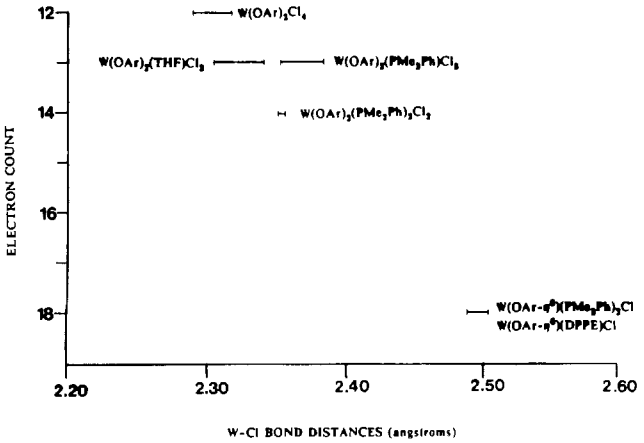

Figure 7. Plot of W-Cl bond distances vs metal electron configuration.

methyl groups, one hydrogen was located in a difference Fourier map, this position was idealized, and the remaining positions were calculated. No hydrogens were refined. No correction for extinction was applied, and there was no decay in the standards. For compound **2** another enantiomorph was resolved, but $R = 0.044$, $R_w = 0.061$, and GOF = 2.358, so the enantiomorph reported here is correct.

$WCl_2(OAr\text{-}2,6\text{-}Ph_2)_2(PMe_2Ph)_2$ (4a). A small, orange crystal was selected and transferred to the goniostat, where it was cooled to −151 °C for characterization and data collection. A systematic search of a limited hemisphere of reciprocal space yielded a set of reflections that exhibited no symmetry or systematic extinctions. The reflections could be indexed on a triclinic lattice, and the choice of the centrosymmetric space group $P\bar{1}$ was confirmed by the subsequent solution and refinement of the structure. The data collection was carried out in the usual manner. A total of 3843 reflections were measured, standard data reduction and averaging resulted in a set of 2839 unique reflections, and 2754 were considered observed by the criterion $F > 3.0\sigma(F)$. The R for the averaging was 0.029 for 944 reflections observed more than once.

The structure was solved by using heavy-atom Fourier techniques. With only one molecule in the asymmetric unit, the molecule had to be situated with the W atom at the origin. All non-hydrogen atoms were located, and following initial refinement all hydrogen atoms were located in a difference map. The full-matrix least-squares refinement was completed by using anisotropic thermal parameters on all non-hydrogen atoms and isotropic thermal parameters on the hydrogen atoms. The final R was 0.034.

The final difference map was essentially featureless, except for a peak of about 1.5 e/Å^3 at the W position. The molecule possesses a crystallographic center of symmetry.

Acknowledgment. We thank the National Science Foundation (Grant CHE-8612063 to I.P.R.) for financial support of this work as well as for support of the Crystallographic Center at Purdue.

Supplementary Material Available: Listings of crystal data and data collection parameters, hydrogen positional and thermal parameters, anisotropic thermal parameters, bond distances and angles, and torsion angles (35 pages); tables of observed and calculated structure factors (80 pages). Ordering information is given on any current masthead page.

Contribution from the Department of Chemistry,
The University of North Carolina at Greensboro, Greensboro, North Carolina 27412

Photosubstitution Reactions of Terpyridine Complexes of Ruthenium(II)

H.-F. Suen, S. W. Wilson, M. Pomerantz, and J. L. Walsh*

Received June 30, 1988

A series of ruthenium-terpyridine complexes, *trans*-Ru(trpy)LCl_2, *cis*-Ru(trpy)L_2Cl^+, Ru(trpy)L_3^{2+} (trpy = 2,2′:6′,2″-terpyridine; L = pyridine (py), acetonitrile, 4-methylpyridine, propionitrile), and *trans*-Ru(trpy)L_2Cl^+ (L = pyridine, 4-methylpyridine), were prepared and characterized by UV-visible and NMR spectroscopy and cyclic voltammetry. In acetone and dichloromethane, Ru(trpy)L_3^{2+} and Ru(trpy)L_2Cl^+ undergo efficient photosubstitution of L by solvent or chloride. For Ru(trpy)$(CH_3CN)_3^{2+}$, Ru(trpy)$(py)_3^{2+}$, *cis*-Ru(trpy)$(CH_3CN)_2Cl^+$, *cis*-Ru(trpy)$(py)_2Cl^+$, and *trans*-Ru(trpy)$(py)_2Cl^+$, $\Phi_{Cl^-} = 0.040, 0.037, 0.127, 0.049$, and 0.0004, respectively; $\Phi_{solvent} = 0.020, 0.004, 0.053, 0.008$, and 0.0002, respectively. Methyl-substituted complexes containing 4-methylpyridine and propionitrile were used to show that L sites were selectively photolabilized and most reactions occurred without rearrangement. The results are discussed in terms of current photosubstitution theories.

Introduction

In studies of photochemical substitution reactions of coordination complexes, it is desirable to be able to predict which ligand is likely to be photolabilized and what rearrangement processes are likely to occur during the substitution process. Models have been developed to predict each of these with varying degrees of success. For d^3 complexes, Adamson's rules have been used to predict ligand labilization.[1] More recently, Vanquickenborne and Ceulemans[2,3] and Wrighton[4] have expanded the concepts of Adamson with a semiempirical model based on the angular overlap model. Models have also been proposed[3,5-7] to explain the rearrangement that occurs following ligand labilization. In general, photolabilization is expected to occur on the axis with the weakest average ligand field to produce a square-pyramidal intermediate. Rearrangement through a trigonal-bipyramidal species may lead to a product with the incoming ligand in a position different from that of the leaving ligand. The occurrence of photosubstitution and isomerization depends on the thermodynamic and kinetic favorability of a number of fundamental steps.

Since (polypyridyl)ruthenium complexes are important as models for solar energy conversion schemes, their photochemical and photophysical properties are of great interest. Photosubstitution is generally undesirable in these schemes; however, an understanding of such reactions is needed to design photostable systems. Photosubstitution in $Ru(bpy)_3^{2+}$[8-10] (bpy = 2,2′-bipyridine), $Ru(bpy)_2L_2^{n+}$,[11-13] and related systems have been studied, but often the bpy ligands place certain constraints on the lability of sites and modes of rearrangement. The ruthenium center in 2,2′;6′,2″-terpyridine (trpy) complexes of ruthenium is

(1) Adamson, A. W. *J. Phys. Chem.* **1967**, *71*, 798.
(2) Vanquickenborne, L. G.; Ceulemans, A. *Coord. Chem. Rev.* **1983**, *157*, and references therein.
(3) Vanquickenborne, L. G.; Ceulemans, A. *J. Am. Chem. Soc.* **1977**, *99*, 2008.
(4) Wrighton, M.; Gray, H. B.; Hammonds, G. S. *Mol. Photochem.* **1973**, *5*, 165.
(5) Vanquickenborne, L. G.; Ceulemans, A. *Inorg. Chem.* **1979**, *18*, 3475.
(6) (a) Purcell, K. F.; Clark, S. F.; Petersen, J. D. *Inorg. Chem.* **1980**, *19*, 2183. (b) Vanquickenborne, L. G.; Ceulemans, A. *Inorg. Chem.* **1978**, *17*, 2730.
(7) Kirk, A. D. *Mol. Photochem.* **1973**, *5*, 127.
(8) Gleria, M.; Minto, F.; Beggiato, G.; Brotolus, P. *J. Chem. Soc., Chem. Commun.* **1978**, 285.
(9) Hoggard, P. E.; Porter, G. B. *J. Am. Chem. Soc.* **1978**, *100*, 1457.
(10) Wallace, W. M.; Hoggard, P. E. *Inorg. Chem.* **1980**, *19*, 2141.
(11) Durham, B.; Walsh, J. L.; Carter, C. L.; Meyer, T. J. *Inorg. Chem.* **1980**, *19*, 860.
(12) (a) Pinnick, D. V.; Durham, B. *Inorg. Chem.* **1984**, *23*, 1440. (b) Pinnick, D. V.; Durham, B. *Inorg. Chem.* **1984**, *23*, 3841.
(13) Caspar, J. V.; Meyer, T. J. *Inorg. Chem.* **1983**, *22*, 2444.

0020-1669/89/1328-0786$01.50/0

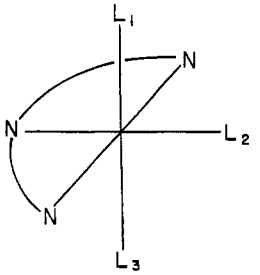

Figure 1. Terpyridine complexes of ruthenium (L_1, L_3 axial; L_2 equatorial; N⌒N⌒N = 2,2′:6′,2″-terpyridine).

analogous to the bpy system but presents an alternate ligand array (see Figure 1—note designation of equatorial and axial positions) with respect to which ligand labilization and rearrangement processes can be studied. The synthesis and photosubstitution reactions of a series of $Ru(trpy)L_2L'^{n+}$ complexes are reported here.

Experimental Section

Preparation of $Ru(trpy)Cl_3$, *trans*-$Ru(trpy)(py)Cl_2$ (py = pyridine), *trans*-$[Ru(trpy)(PPh_3)_2Cl]PF_6$, and *cis*- and *trans*-$Ru(trpy)(PPh_3)Cl_2$ followed literature methods.[14] Acetone and dichloromethane were stored over molecular sieves. Other chemicals were of reagent grade and were used without further purification. Column chromatography was performed with basic aluminum oxide (Aldrich). Elemental analyses were performed by Desert Analytics, Tucson, AZ. Proton NMR spectra were obtained on GE QE-300 or Varian XL-400 spectrometers. Ultraviolet–visible spectra were obtained on a Varian DMS-100 spectrophotometer. A Bioanalytical Systems CV-1B instrument was used to obtain cyclic voltammograms. Emission spectra were obtained on a Perkin-Elmer Model 650-40 fluorescence spectrophotometer.

Preparations. ***trans*-Ru(trpy)(CH_3CN)Cl_2.** To 110 mg (0.25 mmol) of $Ru(trpy)Cl_3$ were added 30 mL of chloroform and 1 mL of acetonitrile. After 1 mL of triethylamine was added, the solution was refluxed for 1.5 h. The mixture was cooled and filtered, and 30 mL of ethanol was added. The solution was reduced in volume to about 20 mL by rotary evaporation and was suction-filtered to collect 56 mg (51%) of purple *trans*-$Ru(trpy)(CH_3CN)Cl_2$. Anal. Calcd for $Ru(C_{15}H_{11}N_3)(CH_3CN)Cl_2$: C, 45.75; H, 3.14; N, 12.55. Found: C, 45.52; H, 3.32; N, 12.25.

***cis*-[Ru(trpy)(CH_3CN)$_2$Cl]PF_6.** To 760 mg (11.27 mmol) of *trans*-$Ru(trpy)(CH_3CN)Cl_2$ was added 250 mL of ethanol/water (1:1) followed by 8 mL of acetonitrile. The mixture was heated at reflux for 20 min, during which time the color changed from purple to red. The mixture was cooled, and the volume was reduced to 100 mL by rotary evaporation. The crude product was precipitated by dropwise addition of a saturated aqueous solution of NH_4PF_6 and then collected by filtration. The crude product mixture, consisting of $[Ru(trpy)(CH_3CN)_3](PF_6)_2$, *cis*-$[Ru(trpy)(CH_3CN)_2Cl]PF_6$, and *trans*-$Ru(trpy)(CH_3CN)Cl_2$, was separated by chromatography. The first fraction, eluted with acetone/dichloromethane (1:1), contained the desired compound. After removal of solvent, the product was dissolved in a minimum volume of acetone, precipitated by adding diethyl ether, and then collected by filtration. Yield: 632 mg (62%). Anal. Calcd for $[Ru(C_{15}H_{11}N_3)(CH_3CN)_2Cl]PF_6$: C, 38.24; H, 2.87; N, 11.73. Found: C, 38.47; H, 3.02; N, 11.53.

[Ru(trpy)(CH_3CN)$_3$]$(PF_6)_2$. To 50 mL of ethanol/water were added 100 mg (0.227 mmol) of $Ru(trpy)Cl_3$ and 2 mL of CH_3CN. After being heated at reflux for 9 h, the solution was reduced in volume to 10 mL by rotary evporation. The product was precipitated by addition of aqueous NH_4PF_6, collected by filtration, and then chromatographed on an alumina column. Yield: 93 mg (55%). Anal. Calcd for $[Ru(C_{15}H_{11}N_3)(CH_3CN)_3](PF_6)_2$: C, 33.75; H, 2.70; N, 11.25. Found: C, 32.81; H, 2.59; N, 11.26.

***trans*-[Ru(trpy)(py)$_2$Cl]PF_6.** To 50 mL of pyridine (py) was added 40 mg (0.060 mmol) of *trans*-$Ru(trpy)(PPh_3)Cl_2$, and the mixture was refluxed for 2 h. After removal of solvent by rotary evaporation, the residue was dissolved in water and the product was precipitated by addition of aqueous NH_4PF_6. The product was collected by filtration, washed with diethyl ether, and air-dried. Yield: 38 mg (95%). Anal. Calcd for $[Ru(C_{15}H_{11}N_3)(C_5H_5N)_2Cl]PF_6$: C, 44.64; H, 3.15; N, 10.41. Found: C, 44.52; H, 3.05; N, 10.22.

***cis*-[Ru(trpy)(py)$_2$Cl]PF_6.** A solution of 150 mg (0.17 mmol) of $[Ru(trpy)(py)_3](PF_6)_2$ in 450 mL of acetone was photolyzed for 70 min. The solution was reduced to a small volume, and the solid was precipitated by addition of diethyl ether. To a solution of 50 mg of the latter solid in 250 mL of acetone was added 10 mg of tetraethylammonium chloride. The volume was reduced by rotary evaporation and the product precipitated by addition of diethyl ether. The product was purified by chromatography on an alumina column. Yield: 34 mg (85%). Anal. Calcd for $[Ru(C_{15}H_{11}N_3)(C_5H_5N)_2Cl]PF_6 \cdot H_2O$: C, 43.45; H, 3.35; N, 10.17. Found: C, 43.95; H, 3.58; N, 9.75.

[Ru(trpy)(py)$_3$]$(PF_6)_2$. This complex was prepared by the same method as for $[Ru(trpy)(CH_3CN)_3](PF_6)_2$. Anal. Calcd for $[Ru(C_{15}H_{11}N_3)(C_5H_5N)_3](PF_6)_2$: C, 41.84; H, 3.04; N, 9.76. Found: C, 42.23; H, 2.95; N, 9.72.

***trans*-[Ru(trpy)(py)$_2$Mepy]$(PF_6)_2$.** To 50 mL of ethanol/water (1:1) were added 50 mg of *trans*-$[Ru(trpy)(py)_2Cl]PF_6$ and a 10-fold molar excess of 4-methylpyridine (Mepy). The solution was refluxed for 4 h. The volume was reduced by rotary evaporation, and the product was precipitated by addition of aqueous NH_4PF_6. The product was collected by filtration and purified by chromatography on an alumina column. Yield: 29 mg (45%). Anal. Calcd for $[Ru(C_{15}H_{11}N_3)(C_5H_5N)_2(C_6H_7N)](PF_6)_2$: C, 42.54; H, 3.22; N, 9.16. Found: C, 42.23; H, 3.18; N, 8.96. The corresponding *trans*-$[Ru(trpy)(Mepy)_2py](PF_6)_2$ complex was prepared by the same method.

***cis*-[Ru(trpy)(CH_3CN)$_2$(CH_3CH_2CN)]$(PF_6)_2$.** A solution of 100 mg of $[Ru(trpy)(CH_3CN)_3](PF_6)$ in 100 mL of acetone was photolyzed with a sunlamp for 50 min. Propionitrile (5 mL) was added, and the solution was rotary-evaporated to about 5 mL. Propionitrile (20 mL) was added again, and the solution was rotary-evaporated to 5 mL. The solution was added to diethyl ether, and the resultant solid was collected by filtration. Yield: 44 mg (43%). The visible spectrum and cyclic voltammogram of the product precisely matched those of $Ru(trpy)(CH_3CN)_3^{2+}$, and the ^1H NMR spectrum exhibited the expected acetonitrile and propionitrile resonances in the appropriate ratio.

Photochemical Methods. Bulk Photolyses. Photolyses were carried out with a 275-W sunlamp and Pyrex glassware. Solutions of the appropriate complex with or without added tetraethylammonium chloride in acetone or dichloromethane were photolyzed while the visible spectrum was monitored by sampling at appropriate intervals. The product was collected by reducing the volume of the solution, precipitating with diethyl ether, and collecting the product by filtration. Column chromatography using alumina was often used to purify the product. Recovery of product was usually greater than 80% of theoretical for the product noted.

Quantum Yield. Quantum yields were measured by using a 200-W Xe–Hg arc lamp housed in a Kratos Model LH150 lamp housing and powered by an LPS251HR lamp power supply. The light beam was focused on an Edmund Scientific interference filter (10-nm band-pass) and then passed onto a quartz spectrophotometer cell (1-cm path length) that was in a cell holder maintained at 25 °C. Incident light intensities were measured by ferrioxalate actinometry. About 3 mL of the sample solution was added to the cell, which was then capped with a rubber syringe cap and flushed with nitrogen. The stirred solution was photolyzed, and the change in composition was monitored by spectral measurement. Reactant concentration was calculated by solution of simultaneous equations. Quantum yields were calculated from the initial slopes of reactant concentration vs time. A standard deviation of 0.003 mol/einstein was typically observed with this method.

Results

Synthesis and Characterization. Substitution of a chloride of $Ru(trpy)Cl_3$ by an incoming ligand (along with ruthenium(III) reduction) resulted in formation of *trans*-$Ru(trpy)LCl_2$ (L = CH_3CN, CH_3CH_2CN, pyridine (py), 4-methylpyridine (Mepy), triphenylphosphine). No evidence for the formation of the cis isomer was obtained. Reaction of *trans*-$Ru(trpy)(CH_3CN)Cl_2$ with CH_3CN in ethanol/water produces a mixture of *cis*-$Ru(trpy)(CH_3CN)_2Cl^+$ and $Ru(trpy)(CH_3CN)_3^{2+}$, which can be separated chromatographically. For the pyridine system, a complex reaction mixture resulted when the analogous reaction was carried out. The complex *trans*-$Ru(trpy)(py)_2Cl^+$ was isolated from the reaction of *trans*-$Ru(trpy)(PPh_3)Cl_2$ with pyridine, a method that also worked well for synthesis of *cis*-$Ru(trpy)(CH_3CN)_2Cl^+$. For the pyridine and acetonitrile systems, $Ru(trpy)L_3^{2+}$ was prepared from $Ru(trpy)LCl_2$ or $Ru(trpy)Cl_3$ by complete substitution of chloride ligands. The other key species in this study, *cis*-$Ru(trpy)(py)_2Cl^+$, was prepared by a photochemical method described later. Attempts to prepare *cis*-Ru-

(14) Sullivan, B. P.; Calvert, J. M.; Meyer, T. J. *Inorg. Chem.* **1980**, *19*, 1404.

Table I. Cyclic Voltammetry and Visible Spectral Data for Terpyridine–Ruthenium Complexes

complex[a]	$E_{1/2}$, V vs SSCE	λ_{max} ($10^{-3}\epsilon$), nm (M^{-1} cm^{-1})
$[Ru(trpy)(AN)_3](PF_6)_2$	1.49[c]	434 (4.4)
$[cis\text{-}Ru(trpy)(AN)_2Cl]PF_6$	0.93[c]	485 (4.6)
$trans\text{-}Ru(trpy)(AN)Cl_2$	0.40[b]	400 (5.3)
		549 (4.8)
$[Ru(trpy)(py)_3](PF_6)_2$	1.26[c]	494 (5.8)
$[cis\text{-}Ru(trpy)(py)_2Cl]PF_6$	0.85[b]	386 (11.2)
		530–550[d] (5.5)
$[trans\text{-}Ru(trpy)(py)_2Cl]PF_6$	0.83[c]	365 (12.8)
		544 (5.7)
$trans\text{-}Ru(trpy)(py)Cl_2$	0.35[b]	395 (8.1)
		562 (5.6)
$[Ru(trpy)(PN)_3](PF_6)_2$	1.54[c]	434 (4.6)
$[cis\text{-}Ru(trpy)(PN)_2Cl]PF_6$	0.93[c]	482 (4.6)
$trans\text{-}Ru(trpy)(PN)Cl_2$	0.38[b]	400 (5.2)
$[Ru(trpy)(Mepy)_3](PF_6)_2$	1.23[c]	502 (5.7)
$[trans\text{-}Ru(trpy)(Mepy)_2Cl]PF_6$	0.78[c]	542 (4.9)
$trans\text{-}Ru(trpy)(Mepy)Cl_2$	0.32[b]	397 (8.0)
		562 (5.7)
$[cis\text{-}Ru(trpy)(PN)_2(AN)](PF_6)_2$	1.49[c]	433 (4.6)
$[cis\text{-}Ru(trpy)(AN)(py)_2](PF_6)_2$	1.29[c]	470 (4.1)
$[cis\text{-}Ru(trpy)(AN)(py)Cl]PF_6$	0.85[c]	367 (7.3)
		508 (4.6)
$[Ru(trpy)(Mepy)(py)_2](PF_6)_2$	1.23[c]	496 (6.0)
$[trans\text{-}Ru(trpy)(py)(PPh_3)Cl]PF_6$	0.86[c]	507 (5.4)

[a] AN = CH_3CN, PN = CH_3CH_2CN. [b] CH_2Cl_2 solution. [c] CH_3CN solution. [d] Broad peak.

$(trpy)LCl_2$ or $trans\text{-}Ru(trpy)(CH_3CN)_2Cl^+$ were unsuccessful.

Synthesis of $trans\text{-}[Ru(trpy)(Mepy)(py)_2](PF_6)_2$ involved substitution of the chloride of $trans\text{-}[Ru(trpy)(py)_2Cl]PF_6$ by Mepy. The proton NMR spectrum of the product confirmed the trans geometry, suggesting that no rearrangement occurred during the thermal substitution in refluxing ethanol/water. For the mixed acetonitrile/propionitrile species $[Ru(trpy)(CH_3CN)(CH_3CN_2CN)_2](PF_6)_2$, the method of Lavallee[15] and Sargeson[16] was used to displace the chlorides from $trans\text{-}Ru(CH_3CN)Cl_2$, followed by reaction with propionitrile. However, proton NMR spectra suggested that substitution resulted in significant scrambling of the acetonitrile between the apical and axial positions. A complex with one propionitrile in the axial position, $cis\text{-}[Ru(trpy)(CH_3CN)_2(CH_3CH_2CN)](PF_6)_2$, was prepared by photolysis of $Ru(trpy)(CH_3CN)_3^{2+}$ followed by reaction with propionitrile.

These terpyridyl complexes show characteristics similar to other (polypyridyl)ruthenium complexes.[17] The absorption spectra are dominated by intense metal-to-ligand charge-transfer (MLCT) bands in the visible region (Table I) and intraligand bands in the UV region ($\lambda_{max} \sim 320, 280$ nm). The MLCT bands are sensitive to the identity of the monodentate ligands and show a regular shift to shorter wavelength as electron density on the metal decreases due to the net donor/acceptor character of the monodentate ligand array. For other (polypyridyl)ruthenium complexes, this shift has been attributed to stabilization of the metal d orbitals by the π-acceptor ligands and a resultant increase in $d-\pi^*$ orbital separation.[17-19] Consistent with this interpretation is the increase in Ru^{III}/Ru^{II} reduction potential as the π-acceptor character of the ligand array increases (Table I).

Proton NMR spectroscopy was used to identify the geometry of the complexes (Table II and supplementary material). Terpyridine resonances in the complexes were assigned by analysis of coupling constants and peak multiplicity and by correlation with the spectrum of the free ligand[20] and other terpyridine complexes.[21]

Table II. Proton NMR Chemical Shift Data[a] for L Ligands of $Ru(trpy)L_{3-n}Cl_n^{(2-n)+}$

complex	CH_3CN equatorial	CH_3CN axial
$trans\text{-}Ru(trpy)(CH_3CN)Cl_2$	2.90 (3, s)	
$cis\text{-}Ru(trpy)(CH_3CN)_2Cl^+$	2.90 (3, s)	2.10 (3, s)
$Ru(trpy)(CH_3CN)_3^{2+}$	2.89 (3, s)	2.17 (6, s)

complex	py H_2	py H_3	py H_4	py H_2	py H_3	py H_4
$trans\text{-}Ru(trpy)(py)Cl_2$	8.50 (2, d)	7.38 (2, t)	7.90 (1, t)			
$trans\text{-}Ru(trpy)(py)_2Cl^+$				7.90 (4, d)	7.05 (4, t)	7.60 (2, t)
$cis\text{-}Ru(trpy)(py)_2Cl^+$	7.82 (2, d)	7.64 (2, t)	8.20 (1, t)	7.75 (2, d)	7.07 (2, t)	7.78 (1, t)
$Ru(trpy)(py)_3^{2+}$	8.40 (2, d)	7.38 (2, t)	7.75 (1, t)	7.57 (4, d)	7.15 (4, t)	7.75 (2, t)

[a] δ (relative area, multiplicity).

For the acetonitrile complexes, only trpy resonances were observable in the aromatic region and assignments could be made reasonably confidently. For the pyridine complexes, the aromatic region was complex but, by comparison with that of acetonitrile and 4-methylpyridine complexes, assignment of proton resonances could be made fairly reliably. Proton resonances for aliphatic protons in coordinated acetonitrile, propionitrile, and 4-methylpyridine were uncomplicated and showed a fairly distinct chemical shift when coordinated in the axial position as opposed to the equatorial position, independent of the identity of other monodentate ligands. For example, $trans\text{-}Ru(trpy)(CH_3CN)Cl_2$, $cis\text{-}Ru(trpy)(CH_3CN)_2Cl^+$, and $Ru(trpy)(CH_3CN)_3^{2+}$ exhibit an equatorial ($\delta = 2.90$, intensity 3), an equatorial and an axial ($\delta = 2.90$, intensity 3; $\delta = 2.10$, intensity 3), and an equatorial and an axial ($\delta = 2.89$, intensity 3; and $\delta = 2.17$, intensity 6) methyl resonance, respectively.

All species were thermally stable except $trans\text{-}Ru(trpy)(CH_3CN)Cl_2$. In acetone, dichloromethane, or chloroform solution, this species decomposed completely at room temperature in a few hours. The decomposition has not been fully characterized but seemed to be more rapid and complete in dilute solution. Decomposition occurred in thoroughly dry solvents and in freeze–thaw-degassed solutions. The complex was stable in acetonitrile but appeared to undergo acetonitrile substitution by solvent in dimethyl sulfoxide. The evidence suggested that acetonitrile is readily lost from $trans\text{-}Ru(trpy)(CH_3CN)Cl_2$ and the resulting intermediate undergoes a complicated decomposition. Spectral changes suggested that $Ru(terpy)Cl_3$ and $cis\text{-}Ru(trpy)(CH_3CN)_2Cl^+$ may be two of the products formed.

Photochemical Results. Photolysis of $Ru(trpy)L_3^{2+}$ or $Ru(trpy)L_2Cl^+$ in low-polarity solvents (acetone or dichloromethane) resulted in efficient loss of L and coordination of a solvent molecule or, in the presence of $N(C_2H_5)_4Cl$, a chloride ion (see Figure 2). The presence of isosbestic points only during early stages of photolysis suggested that a multistep process occurs in each case. Products were isolated, purified by column chromatography, and characterized by visible and ^1H NMR spectroscopy and by cyclic voltammetry. For the acetonitrile system, photolysis in the presence of chloride resulted in the following reactions:

$$Ru(trpy)(CH_3CN)_3^{2+} \xrightarrow[Cl^-]{h\nu} cis\text{-}Ru(trpy)(CH_3CN)_2Cl^+ + CH_3CN$$

$$cis\text{-}Ru(trpy)(CH_3CN)_2Cl^+ \xrightarrow[Cl^-]{h\nu} trans\text{-}Ru(trpy)(CH_3CN)Cl_2 + CH_3CN$$

The second step was confirmed by independent analysis of *cis*-

(15) Anderes, B.; Collins, S. T.; Lavallee, D. K. *Inorg. Chem.* **1984**, *23*, 2203.
(16) Dixon, N. E.; Jackson, W. G.; Lancaster, M. J.; Lawrence, G. A.; Sargeson, A. M. *Inorg. Chem.* **1981**, *20*, 470.
(17) Bryant, G. M.; Fergusson, J. E.; Powell, H. K. J. *Aust. J. Chem.* **1977**, *24*, 257.
(18) (a) Kober, E. M.; Meyer, T. J. *Inorg. Chem.* **1982**, *21*, 3967. (b) Connor, J. A.; Meyer, T. J.; Sullivan, B. P. *Inorg. Chem.* **1979**, *18*, 1388.
(19) Kroener, R.; Heeg, M. J.; Deutsch, E. *Inorg. Chem.* **1988**, *27*, 558.
(20) Lytle, F. E.; Petrosky, L. M.; Carlson, L. R. *Anal. Chim. Acta* **1971**, *57*, 239.
(21) Constable, E. C. *J. Chem. Soc., Dalton Trans.* **1985**, 2687.

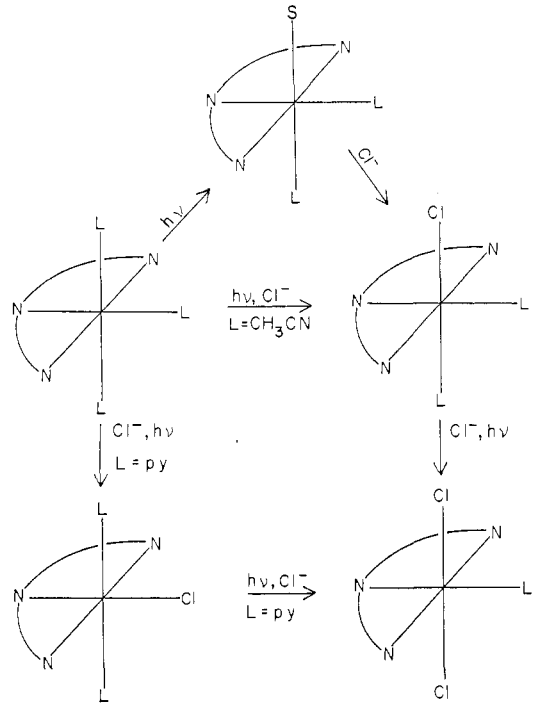

Figure 2. Photosubstitution reactions of terpyridine–ruthenium complexes in acetone solution. L = CH_3CN *or* pyridine except where specifically noted.

$Ru(trpy)(CH_3CN)_2Cl^+$. For the pyridine system, photolysis of $Ru(trpy)(py)_3^{2+}$ in the presence of Cl^- resulted in stepwise formation of *trans*-$Ru(trpy)(py)_2Cl^+$ and then *trans*-$Ru(trpy)(py)Cl_2$. In the absence of added chloride, photolysis of $Ru(trpy)L_3^{2+}$ (L = CH_3CN or py) resulted in formation of a species assumed to be *cis*-$Ru(trpy)L_2S^{2+}$ (S = solvent molecule). This species readily reacted with acetonitrile to produce *cis*-$Ru(trpy)L_2(CH_3CN)^{2+}$ and with chloride to produce *cis*-$Ru(trpy)L_2Cl^+$. Photolysis of *cis*-$Ru(trpy)(CH_3CN)_2Cl^+$ produces $Ru(trpy)(CH_3CN)SCl^+$, which upon substitution by CH_3CN gives *cis*-$Ru(trpy)(CH_3CN)_2Cl^+$ and by chloride gives *trans*-$Ru(trpy)(CH_3CN)Cl_2$. Other photosubstitution reactions were observed during the course of this study and are of related interest. These are summarized by the following equations:

$$\textit{trans}\text{-}Ru(trpy)(PPh_3)_2Cl^+ \xrightarrow[h\nu]{Cl^-} \textit{cis}\text{-}Ru(trpy)(PPh_3)Cl_2$$

$$\textit{cis}\text{-}Ru(trpy)(CH_3CN)_2Cl^+ \xrightarrow[h\nu]{py} Ru(trpy)(CH_3CN)(py)Cl^+ \text{ } (CH_3CN \text{ equatorial})$$

$$\textit{trans}\text{-}Ru(trpy)(py)_2Cl^+ \xrightarrow[h\nu]{CH_3CN} \textit{cis}\text{-}Ru(trpy)(CH_3CN)_2Cl^+$$

To specify the selectivity of photolabilization for axial or equatorial ligands and the possible rearrangements that intermediates may undergo, mixed ligand complexes, *trans*-$Ru(trpy)(Mepy)(py)_2^{2+}$, *trans*-$Ru(trpy)(Mepy)_2(py)^{2+}$, and *cis*-$Ru((trpy)(CH_3CH_2CN)(CH_3CN)_2^{2+}$, were prepared. Spectroscopic results and chemical reactivity suggested that the extra methyl group in each species had minimal effect on the steric and electronic nature of the system. Photolysis of *trans*-$Ru(trpy)(Mepy)(py)_2^{2+}$ in acetone in the presence of $N(C_2H_5)_4Cl$ led to formation of *trans*-$Ru(trpy)(py)_2Cl^+$, on the basis of spectral changes and ^1H NMR data for the isolated product. Photolysis of *trans*-$Ru(trpy)(Mepy)_2(py)^{2+}$ under the same conditions produced an analogous result. When photolyzed in the absence of chloride, *trans*-$Ru(trpy)(Mepy)(py)_2^{2+}$ formed an intermediate that gave *cis*-$Ru(trpy)(Mepy)(py)Cl^+$ (equatorial py) upon reaction with $N(C_2H_5)_4Cl$ in CH_2Cl_2.

Photolysis of $Ru(trpy)(CH_3CN)_3^{2+}$ in propionitrile led to formation of *cis*-$Ru(trpy)(CH_3CN)_2(CH_3CH_2CN)^{2+}$. When this species was isolated and photolyzed in acetone in the presence of $N(C_2H_5)_4Cl$, the NMR spectrum of the product indicated that a significant fraction of the propionitrile was photosubstituted and no propionitrile was observed in the equatorial position. These observations suggest that, except for those of the pyridine complexes in the presence of chloride, the axial ligands are preferentially labilized and no rearrangement occurs during photosubstitution.

Table III. Quantum Yields for Photosubstitution at 25 °C

complex	λ_{irr}, nm	Φ_{Cl^-},[a] mol/einstein	Φ_S,[a] mol/einstein
cis-$Ru(trpy)(AN)_2Cl^+$ [c]	436	0.127	0.053
$Ru(trpy)(AN)_3^{2+}$ [c]	436	0.040	0.020
	480	0.041	
trans-$Ru(trpy)(py)_2Cl^+$ [d]	436	0.0004	0.0002
cis-$Ru(trpy)(py)_2Cl^+$ [d]	436	0.049[b]	0.008
$Ru(trpy)(y))_3^{2+}$ [d]	436	0.037[b]	0.004

[a] Φ_{Cl^-} = quantum yield for the photosubstitution with chloride; Φ_S = quantum yield for the photosubstitution with solvent (S = CH_2Cl_2 or acetone). [b] Quantum yield measurements are dependent on chloride concentration (see text). [c] In dichloromethane. [d] In acetone.

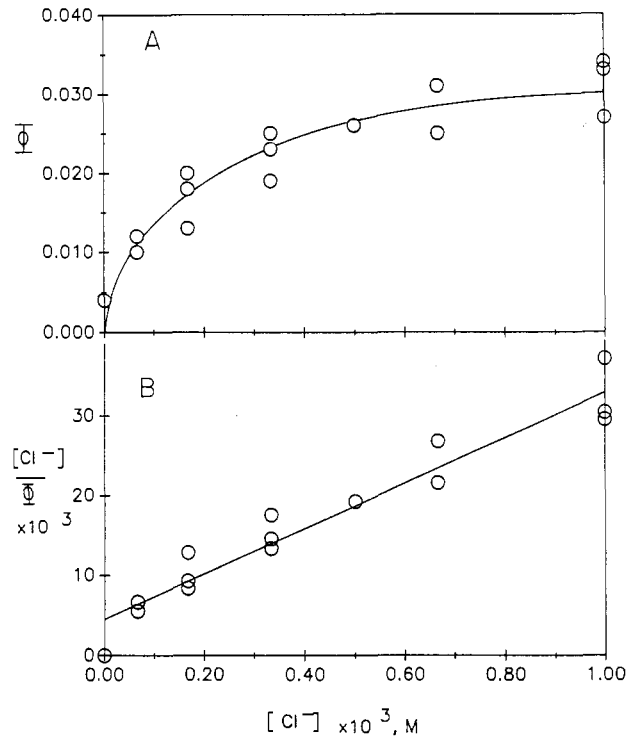

Figure 3. Chloride ion concentration dependence for photosubstitution of $Ru(trpy)(py)_3^{2+}$ in acetone solution.

The photochemical quantum yields for several photosubstitution reactions studied here are given in Table III. The highest quantum yields were observed when $Ru(trpy)L_3^{2+}$ and *cis*-$Ru(trpy)L_2Cl^+$ were photolyzed in the presence of a chloride ion. A much lower quantum yield was observed for *trans*-$Ru(trpy)(py)_2Cl^+$ than for the cis isomer. In the absence of added chloride, quantum yields were smaller than in its presence, particularly for the pyridine species.

Quantum yields were independent of chloride concentration for the acetonitrile complexes but depended on chloride concentration for pyridine complexes in both acetone and dichloromethane. The chloride ion dependence for photosubstitution of $Ru(trpy)(py)_3^{2+}$ is shown in Figure 3. The chloride dependence was interpreted as the result of ion-pair equilibria between the ruthenium complex and chloride ion in the low-polarity solvents used. As such, a plot of $[Cl^-]/\Phi$ vs $[Cl^-]$ is expected to produce a straight line with a slope of $1/\Phi_{ip}$ and an intercept of $1/\Phi_{ip}K_{ip}$, where Φ_{ip} is the quantum yield for photosubstitution within the ion pair and K_{ip} is the ion-pair formation constant.[9] From this analysis, the values of Φ_{ip} and K_{ip} were 0.037 and 6×10^3 for $Ru(trpy)(py)_3^{2+}$ and 0.049 and 9×10^3 for $Ru(trpy)(py)_2Cl^+$.

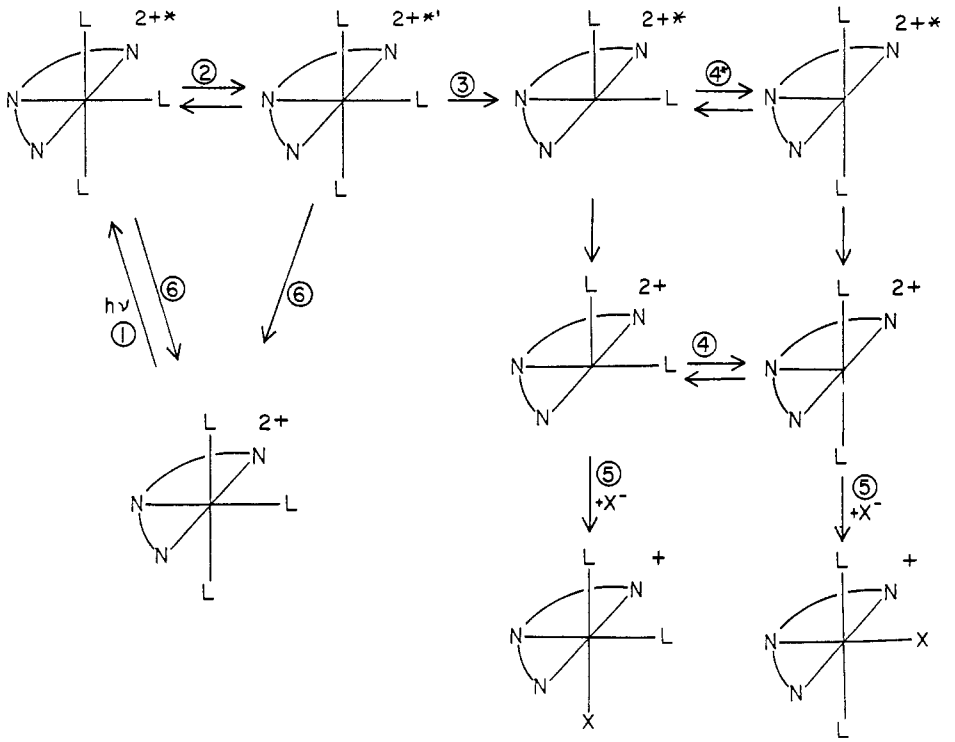

Figure 4. Photosubstitution mechanism for $Ru(trpy)L_3^{2+}$. (* = MLCT excited state; *′ = d–d excited state.)

In acetonitrile solution at room temperature, $[Ru(trpy)(py)_3](PF_6)_2$, *trans*-$[Ru(trpy)(py)_2Cl]PF_6$, and *cis*-$[Ru(trpy)(py)_2Cl]PF_6$ undergo emission at 643, 771, and 725 nm, respectively (with apparently decreasing intensity in the order given), upon excitation near the absorption maximum of the MLCT band. The acetonitrile complexes, $[Ru(trpy)(CH_3CN)_3](PF_6)_2$ and *cis*-$[Ru(trpy)(CH_3CN)_2Cl]PF_6$, showed no room-temperature emission.

Discussion

Terpyridine complexes of ruthenium are of interest because of their close analogy to other (polypyridyl)ruthenium complexes. The terpyridine complexes described here provide a special set of monodentate ligand coordination sites, unlike many (polypyridyl)ruthenium complexes studied. One of the objectives of this study was to develop synthetic techniques for preparation of all possible species in the series *cis*- and *trans*-$Ru(trpy)L_{3-n}Cl_n^{(2-n)+}$ (L = CH_3CN, py; n = 1, 2). Results fell short of that goal, but the species obtained form the basis for an interesting photosubstitution study.

Synthesis. In general, thermal substitution of L for chlorides of $Ru(trpy)Cl_3$ leads to specific geometric isomers for $Ru(trpy)LCl_2$ and $Ru(trpy)L_2Cl^+$, which suggests selective labilization of sites and lack of rearrangement during thermal substitution.

However, results differed for the substitution of acetonitrile or pyridine for a chloride of *trans*-$Ru(trpy)LCl_2$. For the acetonitrile complex, chloride substitution produced *cis*-$Ru(trpy)(CH_3CN)_2Cl^+$, as expected, since thermal substitution reactions of (polypyridyl)ruthenium complexes usually proceed without rearrangement.[14,22] For the pyridine complex, thermal substitution of pyridine for chloride in *trans*-$Ru(trpy)(py)Cl_2$ gave a complex mixture, which suggested that *cis*- and *trans*-$Ru(trpy)(py)_2Cl^+$ and $Ru(trpy)(py)_3^{2+}$ were obtained. Rearrangement may occur to transpose an axial chloride to an equatorial position. The pyridine ligand is sterically more demanding than acetonitrile, and this may be the driving force for rearrangement. With pyridine in the axial positions of *trans*-$Ru(trpy)(py)_2Cl^+$, the hydrogens of the pyridine would not interact with terpyridine hydrogens as they can when the pyridine is equatorial. The reaction of pyridine with *trans*-$Ru(trpy)(PPh_3)Cl_2$ produced *trans*-$Ru(trpy)(py)_2Cl^+$ specifically. Rearrangement must have occurred here, but *trans*-$Ru(trpy)(PPh_3)Cl_2$ is known to isomerize under similar reaction conditions.

Mixed-ligand complexes $Ru(trpy)L_2L'^{n+}$ (L, L′ = py, Mepy, CH_3CN, CH_3CH_2CN, and/or Cl) were prepared by several different methods. Reaction of *trans*-$Ru(trpy)L_2Cl^+$ (L = py, Mepy) with L′ in ethanol/water resulted in L′ substitution for chloride to produce *trans*-$Ru(trpy)L_2L'^{2+}$. Photolysis of $Ru(trpy)L_3^{2+}$ (L = py, CH_3CN, CH_3CH_2CN, Mepy) in acetone resulted in loss of L to produce a labile intermediate,[11,23] presumably *cis*-$Ru(trpy)L_2(acetone)^{2+}$, which readily substituted another ligand for the acetone to produce *cis*-$Ru(trpy)L_2L'^{n+}$.

The possibility of terpyridine acting as a bidentate ligand was considered in analyzing thermal or photochemical reactions. Bidentate terpyridine complexes are known,[24,25] and it is quite possible that a terminal pyridine moiety of the terpyridine ligand may be labilized during thermal or photochemical reactions. However, there was no evidence for this occurring in the reactions studied. If such labilization did take place, recoordination must occur before any observable chemistry can take place. In fact, $Ru(trpy)_2^{2+}$ is photochemically and thermally unreactive under the reaction conditions used in this study.

Excited-State Mechanism. Although details of the excited-state chemistry of the ruthenium–terpyridine complexes reported here are unknown, the results will be discussed on the basis of a tentative model analogous to that of $Ru(trpy)_2^{2+}$,[26-28] $Ru(bpy)_3^{2+}$,[23,29] and $Ru(bpy)_2L_2^{2+}$.[12,13] A simplified scheme is shown in Figure 4. Excitation in the MLCT region presumably leads to a charge-

(22) Chang, J.; Meyerhoffer, S.; Allen, L. R.; Durham, B.; Walsh, J. L. *Inorg. Chem.* **1988**, *27*, 1602.
(23) Durham, B.; Caspar, J. V.; Nagle, J. K.; Meyer, T. J. *J. Am. Chem. Soc.* **1982**, *104*, 4803.
(24) Deacon, G. B.; Patrick, J. M.; Skelton, B. W.; Thomas, N. C.; White, A. H. *Aust. J. Chem.* **1984**, *37*, 929.
(25) Chapman, R. D.; Loda, R. T.; Riehl, J. P.; Schwartz, R. W. *Inorg. Chem.* **1984**, *23*, 1652.
(26) Winkler, J. R.; Netzel, T. L.; Creutz, C.; Sutin, N. *J. Am. Chem. Soc.* **1987**, *109*, 2381.
(27) Kirchhoff, J. R.; McMillin, D. R.; Marnot, P. A.; Sauvage, J. P. *J. Am. Chem. Soc.* **1985**, *107*, 1138.
(28) Stone, M. L.; Crosby, G. A. *Chem. Phys. Lett.* **1981**, *79*, 169.
(29) (a) Van Houten, J.; Watts, R. J. *Inorg. Chem.* **1978**, *17*, 3381. (b) Van Houten, J.; Watts, R. J. *J. Am. Chem. Soc.* **1976**, *98*, 4853.

transfer excited state containing $trpy^{\bullet-}$ (Figure 4, step 1).[26] Low-lying d–d states that lead to photolabilization can be populated from the initial MLCT state[27] (step 2). Nonreactive relaxation to the ground state is shown in step 6. Loss of L (step 3) from either an axial or an equatorial position leads to a 5-coordinate intermediate (only axial labilization is shown). The 5-coordinate intermediate may undergo rearrangement either while still in the excited state (step 4*) or in the ground state (step 4). Ligand capture (step 5) leads to the final product. The net result depends on the occurrence of axial or equatorial labilization and the competitive processes of relaxation, rearrangement, and ligand capture by the 5-coordinate intermediate. Evidence obtained for the terpyridine complexes suggests that usually axial labilization is observed and rearrangement does not occur.

Labilization. Photosubstitution reactions of $Ru(trpy)L_3^{2+}$ cannot provide evidence to identify the site of labilization, since the equatorial and axial ligands are the same. However, NMR analysis before and after photolysis of the methyl-substituted species, $Ru(trpy)L_2L'^{2+}$, allowed identification of whether L or L′ was lost. The analogous process was assumed to occur for $Ru(trpy)L_3^{2+}$. Surprising specificity of ligand loss was observed, and that was usually for the axial site. For $Ru(trpy)(CH_3CN)_3^{2+}$ (with or without chloride present) and $Ru(trpy)(py)_3^{2+}$ (without chloride present), the axial site was labilized almost exclusively (>90% based on isolation of products and NMR analysis). When $Ru(trpy)(py)_3^{2+}$ was photolyzed in the presence of chloride, the equatorial site was preferentially labilized. In this case, the chloride ion may ion-pair specifically in the vicinity of the equatorial pyridine and activate it toward photolabilization. In the absence of chloride in the presence of acetonitrile ligands, the same activation is not present and axial labilization dominates. Chloride ion enhanced the efficiency of pyridine labilization by a factor of 5–10 whereas its effect on acetonitrile labilization was significantly smaller. Chloride ions may be fully ion-paired with acetonitrile complexes by penetrating close to the ruthenium center (vide infra). In the absence of chloride, solvent molecules may penetrate effectively within the pockets between the ligands. Penetration is less effective for bulkier pyridine complexes, with the result of lower photosubstitution quantum yields.

Ligand labilization results are consistent with photosubstitution models,[2] which predict that ligand labilization is expected to occur on the weakest ligand-field axis. Site labilization is surprisingly specific in $Ru(trpy)L_3^{2+}$ even though terpyridine, pyridine, and acetonitrile are similar in ligand-field strength when interacting with the ruthenium(II) center. The axis containing the terminal pyridines of the terpyridine ligand is expected to contain the weakest ligand field because of unfavorable bite angles[24,30] for the terpyridine ligand. No labilization on this axis was observed. Restrictions due to chelation geometry may prevent photolabilization of this site. The central pyridine ring of terpyridine may result in an unusually strong ligand field on that axis because the Ru–N bond is shortened compared to a normal ruthenium–pyridine bond.[24] Thus, the axis containing this bond may be the strong-field axis and therefore not subject to labilization. Axial labilization is then a reasonable expectation for the $Ru(trpy)L_3^{2+}$ complexes.

For *cis*-$Ru(trpy)L_2Cl^+$ complexes, the weak-field axis is the axial axis and loss of axial L to form *trans*-$Ru(trpy)LCl_2$ is expected. High quantum yields were observed for both the acetonitrile and pyridine complexes. For *trans*-$Ru(trpy)(py)_2Cl^+$, the equatorial axis, containing the chloride ligand, is presumably the weak-field axis. Loss of chloride on that axis may result in no net chemistry because rapid thermal recoordination is expected. The central pyridine moiety of terpyridine at the other end of this axis is certainly not subject to labilization. Surprisingly, the lowest quantum yield for loss of L was observed for *trans*-$Ru(trpy)(py)_2Cl^+$. This species lacks an equatorial L but contains two axial L ligands where preferential labilization was usually observed in other species studied.

Rearrangement. Although the constraints imposed by the tridentate terpyridine ligand and the bonding parameters for its interaction with ruthenium are poorly defined, the general concepts[2] of rearrangement during photosubstitution of d^6 complexes probably have some application. According to Figure 4, the 5-coordinate intermediate may rearrange either in its excited-state configuration or in the ground state. Generally, the barrier to ground-state rearrangement is large.[6] Thus, rearrangement is usually controlled by the thermodynamic favorability of the axial-vacant or equatorial-vacant excited-state species and by the kinetic competition between rearrangement and relaxation.

On a thermodynamic basis, the lowest energy square-pyramidal species is one with a weak σ-donor in the apical position and the strong σ-donors in the equatorial positions.[6] For the $Ru(trpy)L_3^{2+}$ complexes studied, the ligand-field strength is probably fairly similar at all sites and no rearrangement is expected. The studies with methyl-substituted pyridine and acetonitrile ligands show that the observed products were the result of specific site labilization and rearrangement did not occur. For *cis*-$Ru(trpy)L_2Cl^+$ complexes, the intermediate with an apical chloride is predicted to be lowest in energy and a trans product is expected. However, axial labilization, as observed, would naturally lead to a trans product without rearrangement. Rearrangement does occur during the photosubstitution of chloride for pyridine in *trans*-$Ru(trpy)(py)_2Cl^+$ and during the photosubstitution of both pyridines of *trans*-$Ru(trpy)(py)_2Cl^+$ by acetonitrile. Each observation is consistent with rearrangement of the initially formed 5-coordinate intermediate with basal chloride to produce the intermediate with an apical chloride.

Emission. The efficiency of excited-state emission from terpyridine–ruthenium complexes has been related to the ability of solvent molecules to penetrate into pockets between the ligands.[27] The lack of room-temperature emission from $Ru(trpy)(CH_3CN)_3^{2+}$ and *cis*-$Ru(trpy)(CH_3CN)_2Cl^+$ may result from efficient excited-state quenching by solvent interaction. The complexes with sterically more demanding pyridine ligands may preclude short-range solvent interaction, resulting in more efficient room-temperature emission. Alternately, the acetonitrile ligands will raise the energy of the MLCT state and lower or minimally affect the d–d state. Thus, more efficient relaxation to a low-lying d–d state for the acetonitrile complexes may prevent significant occupation of the emitting MLCT state. Such an explanation has been applied to $Ru(bpy)_2L_2^{2+}$ species.[12]

Summary. Photosubstitution in $Ru(trpy)L_3^{2+}$ and $Ru(trpy)L_2Cl^+$ occurs efficiently with surprising specificity in site labilization. The labilization and rearrangement (or lack thereof) can be reasonably well explained by present photosubstitution theory based on the angular overlap model.

Acknowledgment. We thank the donors of the Petroleum Research fund, administered by the American Chemical Society, and the UNC-Greensboro Research Council for financial support of this research. The assistance of Prof. Paul Rillema and the Department of Chemistry at UNC-Charlotte in obtaining NMR and emission spectra is gratefully acknowledged.

Supplementary Material Available: Table IV, listing assignments of proton NMR spectra (3 pages). Ordering information is given on any current masthead page.

(30) Constable, E. C. *Adv. Inorg. Chem. Radiochem.* **1986**, *30*, 69.